Noname manuscript No.
(will be inserted by the editor)

Narrowband Solid State VUV Coherent Source for Laser Cooling of Antihydrogen

J. Mario Michan · Gene Polovy · Kirk W. Madison · Makoto C. Fujiwara · Takamasa Momose*

Received: date / Accepted: date

Abstract We describe the design and performance of a solid-state pulsed source of narrowband (< 100 MHz) Lyman-α radiation designed for the purpose of laser cooling magnetically trapped antihydrogen. Our source utilizes an injection seeded Ti:Sapphire amplifier cavity to generate intense radiation at 729.4 nm, which is then sent through a frequency doubling stage and a frequency tripling stage to generate 121.56 nm light. Although the pulse energy at 121.56 nm is currently limited to 12 nJ with a repetition rate of 10 Hz, we expect to obtain greater than 0.1 μJ per pulse at 10 Hz by further optimizing the alignment of the pulse amplifier and the efficiency of the frequency tripling stage. Such a power will be sufficient for cooling a trapped antihydrogen atom from 500 mK to 20 mK.

Keywords Lyman-Alpha · VUV · Antihydrogen · Laser Cooling

1 Introduction

As the simplest and best understood atom in the periodic table, hydrogen appeared to be the natural choice for early laser cooling experiments. Despite this, the first and only study of the optical cooling of hydrogen was published in 1993 [16], many years after several alkalis were successfully cooled and trapped. The reason for this is the inherent difficulty of producing coherent radiation at the

J. M. Michan, M. C. Fujiwara
TRIUMF
4004 Wesbrook Mall, Vancouver, BC Canada V6T 2A3

G. Polovy, and K. W. Madison
Department of Physics and Astronomy, The University of British Columbia
6224 Agricultural Road, Vancouver, BC Canada V6T 1Z1

T. Momose
Department of Chemistry, Department of Physics and Astronomy, The University of British Columbia,
2036 Main Mall, Vancouver, BC Canada V6T 1Z1
Tel.: +1-604-822-5401
Fax: +1-604-822-2847
E-mail: momose@chem.ubc.ca

laser cooling transition for hydrogen - 121.56 nm or Lyman-α. Numerous broadband pulsed Lyman-α sources were developed in the late 1970s and early 1980s [2, 4, 9–13, 17]. These were suitable for many spectroscopic applications, but not for laser cooling, which requires, for efficient cooling, the linewidth of the source to be less than or equal to the natural linewidth ($\Gamma \approx 100$ MHz) of the transition [16]. The first narrowband ($\Delta\nu \approx 40$ MHz) Lyman-α source was developed in 1987 [3] based on non-resonant third-harmonic generation of frequency-doubled pulse-amplified light from a tunable CW dye laser, which made it possible to laser cool hydrogen, trapped in a magnetic trap, to less than 8 mK [16]. Nevertheless, low repetition rate pulsed sources cannot be used for conventional laser cooling experiments, which rely on optical molases, and interest in coherent Lyman-α sources subsided until a new application emerged - laser cooling of trapped antihydrogen. In particular, the ALPHA collaboration at CERN successfully trapped antihydrogen in a magnetic trap at a translational temperature of 500 mK and plans to use the trapped antimatter to test for charge, parity and time (CPT) symmetry violations and to investigate matter-antimatter gravity interactions [1, 5]. To reach the level of accuracy required for these measurements, the trapped antihydrogen must be cooled to a translation temperature of ~ 20 mK. According to simulations [5], a high power (~ 1 μW) Lyman-α source with a 100 MHz linewidth is required to perform the antihydrogen cooling. Two continuous wave (CW) Lyman-α sources, which rely on a four-wave mixing scheme in mercury vapour, have been realized [8, 15], but they are not yet capable of delivering sufficient power (and one of them relies on dye lasers). Here, we present an alternative approach - a narrowband (< 100 MHz) pulsed solid-state Lyman-α source. Our motivation was to develop a completely solid-state source to avoid the maintenance and additional safety issues associated with a dye-laser-based source. Simulations have shown that a narrowband pulsed source that produces 0.1 μJ per shot at a repetition rate of 10 Hz is capable of cooling a trapped antihydrogen atom down to 20 mK [5]. The goal of our development is to achieve this level of 121.56 nm pulse energy with a solid-state laser system.

2 Apparatus

The laser system shown in Fig. 1 consists of a pulsed Ti:Sapphire amplifier seeded by a narrow linewidth (< 1 MHz) semiconductor laser (Toptica Photonics TA Pro) operating at 729.4 nm, an anti-reflection coated type I BBO crystal (Castech Inc.) for second harmonic generation (SHG) at 729.4 nm and a third harmonic generation (THG) and detection chamber.

2.1 Ti:Sapphire Amplifier and SHG

To obtain the intensities required for efficient SHG and THG while maintaining a narrow linewidth, we used an injection seeded pulsed Ti:Sapphire amplifier based on [7]. This amplifier is an unstable resonator that consists of two Brewster cut Ti:Sapphire crystals (10 mm in diameter, 36.8 mm in path length, GT Advanced Technologies), a convex graded reflectivity mirror (f = −5 m, INO) coated for 729.4 nm, a high reflector (HR) and two isosceles Brewster prisms for coarse

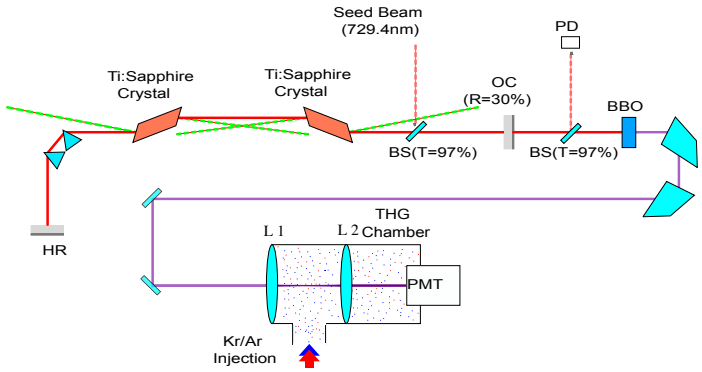

Fig. 1 Laser arrangement and non-linear optical stages. The Ti:Sapphire amplifier cavity is seeded by a narrow linewidth semiconductor laser via an uncoated CaF_2 beam splitter (BS) with a reflectivity of $\sim 3\%$. The two Ti:Sapphire crystals are pumped from both sides by a pulsed Nd:YAG laser. The pump power is distributed evenly between the four arms. The amplified light, which exits the cavity via the output coupler (OC), is then sent through a coated BBO crystal. The second harmonic is separated from the fundamental beam (not shown), with two Pellin Broca prisms and routed to the THG chamber. The beam is then focused by an MgF_2 lens L_1 ($f = 100$ mm) onto a mixture of krypton and argon gas. Finally, Lyman-α radiation is produced by non-resonant THG, recollimated by an MgF_2 lens L_2 ($f = 200$ mm) and detected by a solar-blind photo-multiplier tube (PMT). Two Lyman-α filters are placed between L_2 and the PMT to prevent 364.7 nm light from reaching the PMT (not shown).

wavelength selection. As demonstrated previously in [7], the generation of the Fourier-limit pulses can be achieved when each crystal is pumped by a pulsed frequency doubled Nd:YAG laser (532 nm, 10 Hz repetition rate) from both sides and injection seeded with a CW diode laser ($\Delta\nu < 1$ MHz, 729.4 nm). The output of the amplifier is then sent into a coated type I BBO crystal (dimensions: 7 mm $\times$ 7 mm $\times$ 8 mm), to produce 364.7 nm radiation. After the second harmonic (364.7 nm) is spatially separated from the fundamental beam (729.4 nm) by means of two Pellin Broca prisms, it is sent to the THG chamber, where we produce and detect Lyman-α radiation.

2.2 Lyman-α Generation and Detection

To generate Lyman-α radiation, we used non-resonant THG in a mixture of krypton and argon - an approach that has been demonstrated a number of times in the literature [2–4,9,10,12,17]. A resonant four-wave-mixing (FWM) scheme was also successfully demonstrated with a broadband dye-laser source by Michan et al. [14]. However, THG (which requires only one color) was chosen here because of its technical simplicity and the availability of high energy pump sources. In Fig. 1, we show that radiation from the SHG stage is sent into the THG chamber, which consists of an MgF_2 focusing lens L_1 ($f = 100$ mm), an input port for the krypton-argon mixture, an MgF_2 recollimating lens L_2 ($f = 200$ mm), two Lyman-α filters (Pelham Research Optical L.L.C. 122-NB) and a solar-blind photo-multiplier tube (PMT: Hamamatsu R972). In our implementation, the first lens L_1 focuses the

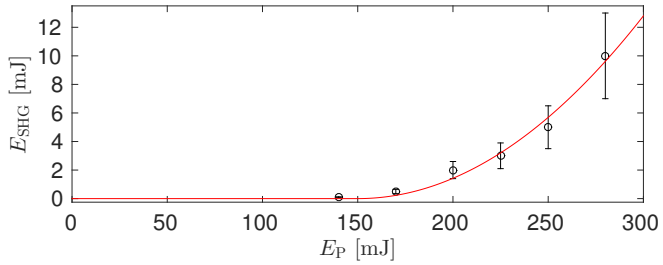

Fig. 2 SHG pulse energy at 365 nm as a function of the pulse energy of the 532 nm pump for the 729.4 nm seeded amplifier.

slowly diverging 364.7 nm beam (with a vertical diameter of 6 mm and a horizontal diameter of 3 mm at 3 m away from the BBO crystal, based on a burn card measurement) onto the gas mixture to reach the intensities required for efficient THG. The generated Lyman-α is then recollimated with lens L_2, sent through two Lyman-α filters (to prevent the 364.7 nm pulses from reaching the detector) and detected by the PMT. Using the response function, gain curve and quantum efficiency of the PMT (Hamamatsu R972) we extract from the raw signal the temporal profile of the Lyman-α beam and its pulse energy. To confirm the production of Lyman-α, we verified that the PMT signal vanished completely in the absence of krypton in the THG chamber.

3 Results

In this section, we describe the results we obtained at the SHG and THG stages. A detailed description and characterization of the injection seeded Ti:Sapphire amplifier can be found in [7] and [6].

3.1 Second Harmonic Generation Stage

3.1.1 Pulse Energy

In Fig. 2, the average pulse energy of the second harmonic (364.7 nm) E_{SHG} is plotted as a function of the 532 nm pump pulse energy E_{P}. This data was taken with the cavity of the Ti:Sapphire amplifier unlocked (free run), and therefore large fluctuations in the pulse-to-pulse energy were observed due to the fluctuation of the cavity length. We fit this data to the following model:

$$E_{\mathrm{SHG}} = \alpha \cdot (E_{\mathrm{P}} - E_{\mathrm{TH}})^2 \cdot \Theta\,(E_{\mathrm{P}} - E_{\mathrm{TH}}) \tag{1}$$

where $\alpha = (5.7 \pm 2.8) \times 10^{-4}\mathrm{mJ}^{-1}$ is a proportionality constant, $E_{\mathrm{TH}} = 150 \pm 27$ mJ is the pump power at the 729.4 nm lasing threshold and Θ is the Heaviside step function.
Further optimizations of the alignments of the amplifier cavity and pump geometries enabled us to reach the SHG pulse energies shown in Fig. 3 with $E_{\mathrm{P}} = 310$ mJ, where the mean pulse energy is 16.0 mJ and the standard deviation is 1.4 mJ. In

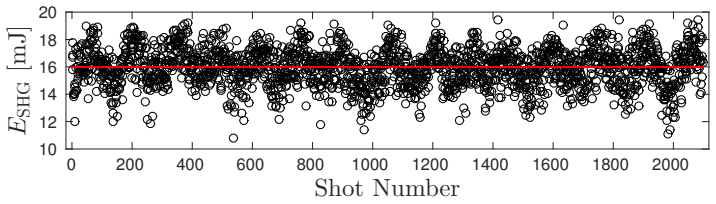

Fig. 3 SHG pulse energy with $E_{\mathrm{P}} = 310$ mJ as a function of time with the amplifier cavity locked. The mean pulse energy is 16.0 mJ and the standard deviation is 1.4 mJ.

this example, the amplifier cavity was locked to off-resonance with the seed frequency, in which the transmittance of the seed laser radiation from the cavity was near the minimum. A slow fluctuation (~ 20 sec) in the pulse energy seen in Fig. 3 might be due to the temperature fluctuation of the BBO crystal, which will be removed in the near future.

3.1.2 Pulse Shape

Fig. 4 (a) and (b), respectively, shows an instantaneous intensity (arbitrary units) of a 364.7 nm pulse as a function of time and the corresponding spectrum when the amplifier cavity was near-resonance with the seed frequency, in which the transmittance of the seed laser radiation from the cavity was near the maximum. The spectrum (b), which is obtained by taking a Fourier transform of the temporal profile shown in (a), consists of a dominant peak (which corresponds to the envelope of the temporal profile) and two side lobes, which account for the modulation seen in the temporal profile. Since a simple side-locking technique was employed for the cavity locking, there were still a non-negligible detuning of the cavity length with respect to the seed laser wavelength, which resulted in the excitation of the adjacent cavity mode via the mode coupling [7]. The frequency separation between the dominant peak and the side lobe is about 95 MHz, which roughly corresponds to the free spectral range (FSR) of the cavity (length ~ 1.55 m). The full width at half maximum (FWHM) of the temporal profile Δt_{FWHM} and the FWHM of the spectrum $\Delta\nu_{\mathrm{FWHM}}$ are 20.9 ± 3.0 ns and 44.3 ± 2.1 MHz, respectively. Similarly, the temporal profile and spectrum of a pulse generated when the amplifier cavity is off-resonance with the seed frequency are shown in Fig. 5 (a) and (b). When the amplifier cavity was off-resonance, the side-bands were more enhanced, which account for the deeper modulation seen in the temporal profile. For this pulse, $\Delta t_{\mathrm{FWHM}} = 21.3 \pm 2.0$ ns and $\Delta\nu_{\mathrm{FWHM}} = 42.7 \pm 1.4$ MHz. The pulse energy at 364.7 nm is 5.0 mJ and 7.2 mJ at 250 mJ pump energy (532 nm) for the near-resonant (Fig. 4) and off-resonant (Fig. 5) conditions, respectively. The off-resonant cavity condition results in higher total pulse energy than the near-resonant condition due to the stronger mode coupling, which was also reported in [7].

3.2 THG Stage

The Lyman-α power is proportional to $\chi^2 N^2 I_{\mathrm{SHG}}^3 F$, where χ is the third order susceptibility, N is the number density of the krypton, I_{SHG} is the power of the

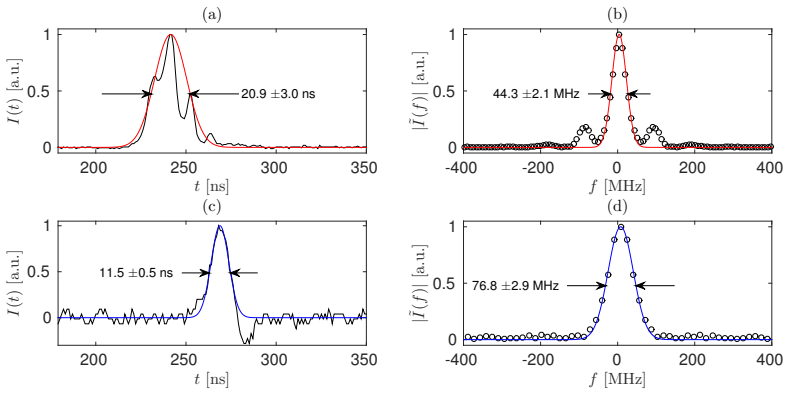

Fig. 4 Temporal and spectral profiles of the 364.7 nm and 121.56 nm pulses with the amplifier cavity locked to near-resonance with the seed laser. (a) Temporal profile of a single pulse at 364.7 nm. Black: Observed intensity. Red: Fitted curve with a Gaussian function. (b) Spectral profile of the 364.7 nm pulse. Black: Fourier transform of the black trace in (a). Red: Fitted curve with a Gaussian function. (c) Temporal profile of the 121.56 nm pulse. Black: Observed intensity. Red: Fitted curve with a Gaussian function.(d) Spectral profile of the 121.56 nm pulse. Black: Fourier transform of the black trace in (a). Red: Fitted curve with a Gaussian function.

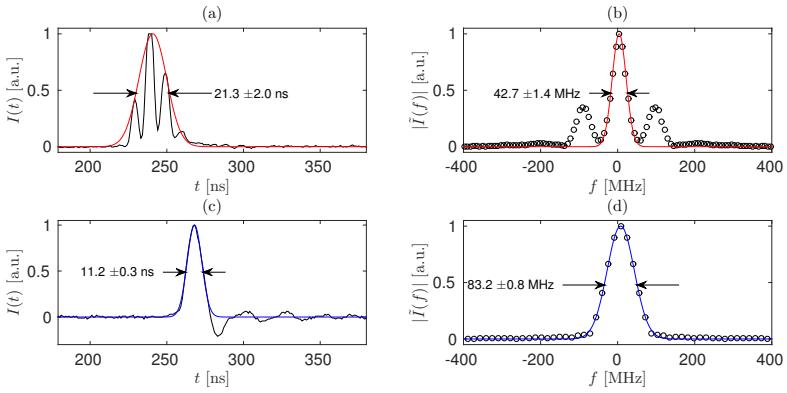

Fig. 5 Temporal and spectral profiles of the 364.7 nm ((a) and (b)) and 121.56 nm ((c) and (d)) pulses with the amplifier cavity locked to off-resonance with the seed laser. See the caption of Fig. 4.

364.7 nm beam and F is the phase matching factor. In the limit of a tight focus, the phase-matching factor is maximized when $b \cdot \Delta k = b \cdot (k_{121.56\ \mathrm{nm}} - 3 \cdot k_{364.7\ \mathrm{nm}}) = -2$, where b is the confocal parameter of the beam (assuming a TEM_{00} mode) [9]. However, because the Lyman-α power is also proportional to N^2, adjusting the krypton density to satisfy the phase matching condition alone is insufficient to optimizing the Lyman-α power and the problem becomes a three parameter optimization for the focal length of the focusing lens L_1 and the pressures of krypton and argon in the mixing chamber. Based on previous results from preliminary dye-laser experiments and some empirical optimization, we chose an f = 100 mm MgF_2 lens for L_1 and set the krypton pressure to 84 mTorr and the argon pressure

to 200 mTorr for the present study.

With the amplifier cavity locked to the near-resonance, we observed the temporal profile for the 121.6 nm pulse as shown in Fig. 4 (c). The corresponding spectrum shown in Fig. 4 (d) is obtained by the Fourier transform of the temporal profile in (c). The generated Lyman-α pulse has a temporal width of $\Delta t_{\mathrm{FWHM}} = 11.5 \pm 0.5$ ns and a spectral width of 76.8 ± 2.9 MHz. Note that the temporal width of the 121.56 nm pulse in (c) might be slightly broadened due to the response time of the PMT (the anode pulse rise time of 1.6 ns and the electron transit time of 17 ns). As a result, the spectral width obtained in (d) might be slightly narrower than the actual spectral width. Corresponding temporal profile and spectrum for the 121.6 nm pulse with the off-resonant cavity condition are shown in Fig 5 (c) and (d), respectively. The generated 121.56 nm pulse has similar temporal and spectral profiles; $\Delta t_{\mathrm{FWHM}} = 11.2 \pm 0.3$ ns and $\Delta \nu = 83.2 \pm 0.8$ MHz. The spectral width is slightly broadened with this condition.

Remarkably, we found that locking the cavity in the off-resonant condition with the seed laser resulted in higher THG efficiency than the cavity in the near-resonant condition. At 250 mJ of 532 nm pump energy, the off-resonant condition shown in Fig. 5 resulted in 12 nJ pulse energy for the 121.46 nm pulse. On the other hand, the near-resonant condition shown in Fig. 4 resulted in only 2 nJ pulse energy for the 121.46 nm pulse. The higher THG efficiency with the off-resonant condition is most likely due to the higher peak power density of each pulses in the pulse train at 364.7 nm shown in Fig. 5 (a). For the laser cooling of antihydrogen, whose whose natural linewidth is expected to be $\Gamma \approx 100$ MHz, the off-resonant condition for the amplifier cavity would be better than the near-resonant condition because of the higher pulse energy at 121.46 nm.

4 Conclusion and Outlook

Here, we have developed a solid-state pulsed source of narrowband (< 100 MHz) Lyman-α radiation. The maximum Lyman-α output we have demonstrated here - by frequency tripling a 7.2 mJ pulse of 364.7 nm light - was 12 nJ. Due to the present environmental conditions (humidity and temperature) of the facility, we were forced to lower the pulse energy of 532 nm in order to avoid any optical damage on the Ti:Sapphire crystals. For this reason, the data presented in Sec. 3.2 were taken at the 532 nm pump energy of 250 mJ. Since we have observed about 20 mJ of 364.7 nm radiation as the maximum energy of a single shot at the 532 nm pump energy of 310 mJ (Figs. 2 and 3), we are confident that, after alleviating problems due to the environment, more than 0.1 μJ is possible with this system. The pulse energy at 121.5 nm generated by THG is proportional to the cube of the pulse energy at 364.7 nm, and therefore, if the conversion efficiency remains constant, simply increasing the SHG pulse energy to 20 mJ would result in approximately 0.26 μJ of Lyman-α. In addition, further improvement of the THG conversion efficiency would be expected by optimizing the krypton and argon pressures in the THG chamber and the focal length of the focusing lens (L_1) in order to achieve better phase matching condition for the THG process. While we have made significant progress toward developing a narrowband solid state Lyman-α source, further optimization of the present system will be required to achieve sufficient pulse energies with stable operation in order to use this Lyman-

α source for laser cooling trapped antihydrogen, from 500 mK to 20 mK. Further development is underway.

5 Acknowledgements

We acknowledge Prof. Terry Miller at Ohio State University and his group members for providing us technical details of their pulse amplifier system. The present work was supported by a National Science and Engineering Research Subatomic Physics Project Grant in Canada and funds from Canada Foundation for Innovation for the Centre for Research on Ultra-Cold Systems (CRUCS) at UBC.

References

1. Andresen, G., Ashkezari, M., Baquero-Ruiz, M., Bertsche, W., Bowe, P.D., Butler, E., Cesar, C., Chapman, S., Charlton, M., Deller, A., et al.: Trapped antihydrogen. Nature **468**(7324), 673–676 (2010)
2. Batishche, S., Burakov, V., Kostenich, Y., Mostovnikov, V., Naumenkov, P., Tarasenko, N., Gladushchak, V., Moshkalev, S., Razdobarin, G., Semenov, V., Shreider, E.: Optimal conditions for third-harmonic generation in gas mixtures. Optics Communications **38**(1), 71 – 74 (1981)
3. Cabaret, L., Delsart, C., Blondel, C.: High resolution spectroscopy of the hydrogen lyman-α line stark structure using a vuv single mode pulsed laser system. Optics Communications **61**(2), 116 – 119 (1987)
4. Cotter, D.: Tunable narrow-band coherent VUV source for the lyman-alpha region. Optics Communications **31**(3), 397 – 400 (1979)
5. Donnan, P.H., Fujiwara, M.C., Robicheaux, F.: A proposal for laser cooling antihydrogen atoms. Journal of Physics B: Atomic, Molecular and Optical Physics **46**(2), 025,302 (2013)
6. Dupré, P.: Modeling a nanosecond quasi-fourier-transform limited ti: Sa laser source. The European Physical Journal Applied Physics **40**(03), 275–291 (2007)
7. Dupré, P., Miller, T.A.: Quasi-fourier-transform limited, scannable, high energy titanium-sapphire laser source for high resolution spectroscopy. Review of Scientific Instruments **78**(3), 033102 (2007)
8. Eikema, K.S.E., Walz, J., Hänsch, T.W.: Continuous wave coherent lyman-α radiation. Phys. Rev. Lett. **83**, 3828–3831 (1999)
9. Hilbig, R., Wallenstein, R.: Enhanced production of tunable vuv radiation by phase-matched frequency tripling in krypton and xenon. Quantum Electronics, IEEE Journal of **17**(8), 1566–1573 (1981)
10. Langer, H., Puell, H., Röhr, H.: Lyman alpha (1216 å) generation in krypton. Optics Communications **34**(1), 137 – 142 (1980)
11. Mahon, R., Tomkins, F.S., Kelleher, D.E., McIlrath, T.J.: Four-wave sum mixing in beryllium around hydrogen lyman-α. Opt. Lett. **4**(11), 360–362 (1979)
12. Mahon, R., Yiu, Y.M.: Generation of lyman-α radiation in phase-matched rare-gas mixtures. Opt. Lett. **5**(7), 279–281 (1980)
13. McKee, T.J., Stoicheff, B.P., Wallace, S.C.: Tunable, coherent radiation in the lyman-α region (1210–1290 å) using magnesium vapor. Opt. Lett. **3**(6), 207–208 (1978)
14. Michan, J.M., Fujiwara, M.C., Momose, T.: Development of a lyman-α laser system for spectroscopy and laser cooling of antihydrogen. Hyperfine Interactions **228**(1-3), 77–80 (2014)
15. Scheid, M., Kolbe, D., Markert, F., Hänsch, T.W., Walz, J.: Continuous-wave lyman-α generation with solid-state lasers. Opt. Express **17**(14), 11,274–11,280 (2009)
16. Setija, I.D., Werij, H.G.C., Luiten, O.J., Reynolds, M.W., Hijmans, T.W., Walraven, J.T.M.: Optical cooling of atomic hydrogen in a magnetic trap. Phys. Rev. Lett. **70**, 2257–2260 (1993)
17. Wallenstein, R.: Generation of narrowband tunable VUV radiation at the lyman-α wavelength. Optics Communications **33**(1), 119 – 122 (1980)